Interlocked attosecond pulse trains in slightly bi-elliptical high harmonic generation

IOP Publishing J. Phys. Photonics 2 (2020) 034005 https://doi.org/10.1088/2515-7647/ab8a5c

Journal of Physics: Photonics

OPEN ACCESS

RECEIVED
29 December 2019

REVISED
30 March 2020

ACCEPTED FOR PUBLICATION
17 April 2020

PUBLISHED
27 May 2020

PAPER

Interlocked attosecond pulse trains in slightly bi-elliptical high harmonic generation

Eliyahu Bordo[1], Ofer Kfir[2], Sergey Zayko[2], Ofer Neufeld[1], Avner Fleischer[3,4], Claus Ropers[2,5] and Oren Cohen[1]

[1] Solid State Institute and Physics Department, Technion – Israel Institute of Technology, Haifa 3200003, Israel
[2] 4th Physical Institute, University of Göttingen, Göttingen 37077, Germany
[3] Raymond and Beverly Sackler Faculty of Exact Science, School of Chemistry, Tel Aviv University, Tel-Aviv 6997801, Israel
[4] Tel-Aviv University Center for Light-Matter-Interaction, Tel Aviv 6997801, Israel
[5] International Center for Advanced Studies of Energy Conversion (ICASEC), University of Göttingen, Göttingen, Germany

E-mail: elibordo@technion.ac.il **and** oren@technion.ac.il

Keywords: bi-elliptical high harmonic generation, attosecond pulse trains, ellipticity-resolved spectroscopy

Supplementary material for this article is available online

Abstract

The ellipticity of high harmonics driven by bi-chromatic (e.g. $\omega - 2\omega$) co-propagating fields can be fully tuned by varying the polarization of the pump components. In order to start revealing the underlying mechanism of this control, we explore a relatively simple regime of this scheme that still gives rise to full control over the harmonics ellipticities. In this regime, the pumps are only slightly elliptical and the high harmonic radiation consists of two (different) interlocked attosecond pulse trains (APTs). We formulate a semi-analytic model that maps the high harmonic ellipticity to properties of the APTs harmonic decompositions. Utilizing this model, we reconstruct these APTs variables from measurements of the high harmonics ellipticities. This ellipticity-resolved spectroscopy of interlocked APTs may be useful for ultrafast probing of chiral degrees of freedom.

Several experimental techniques for generation of highly helically polarized high-order harmonics [1–10] have been recently demonstrated to overcome the historical limitation to linearly polarized high harmonic generation (HHG) process. In the first demonstration, which followed a proposal in 1995 [11–13], circularly polarized high harmonics were generated by co-propagating bi-chromatic ($\omega - 2\omega$) circularly-polarized pumps (bi-circular pumps) that interacted with isotropic gas [1]. This generation technique gave rise to various experimental applications, including investigation of spin mixing [1, 14, 15], spin-orbit interaction [16] and conservation of Torus-knot angular momentum [17] in HHG, probing rotational symmetry in aligned molecules [18], population of laser-driven Rydberg states [19], molecular chirality [20, 21], magnetic circular dichroism [2, 5] and nanoscale magnetic imaging [22]. Generation of bright highly helically polarized harmonics was reported using $\omega - 2\omega$ pumps that are cross linearly polarized and interacted with gas composed of atoms with p-shell valence states [6, 23, 24]. Interestingly, the half-wave dynamical reflection symmetry in this scheme [25] (which is not broken by the fact that the valance electrons are initially in p-states [26]) is expected to yield only linearly polarized high harmonics (the odd and even harmonics are polarized along the polarization axes of the ω and 2ω drivers, respectively) [27, 28].

The polarization of high harmonics driven by bi-circular, bi-parallel and crossed-linear bi-chromatic pumps in isotropic media are determined by the selection rules of these high symmetry systems [25]. In the bi-circular case, the ellipticities of the $3n+1$ ($n = 1, 2, 3, \ldots$) and $3n-1$ harmonics are circular, with helicities like the ω and 2ω pump components, respectively [12, 13, 29]. In the time domain, three interlocked attosecond pulse trains (APTs) are emitted, where each APT is $T/3$ time shifted (T is the optical cycle of the ω pump component) and $2\pi/3$ polarization rotated with respect to the preceding APT [30, 31]. Other than these two changes, the APTs are identical (neglecting envelope effects). In the cross linear case, the odd and even harmonics are polarized linearly along the polarization axes of the ω and 2ω drivers, respectively [27, 28]. In the time-domain, two interlocked APTs are emitted with $T/2$ delay between them (a $\pi/2$ relative phase between the pump components leads to re-collisions of only the short electronic trajectories [32, 33]). The angle between the polarization axes of the APTs is chirped [34–36] and is

determined by the intensity ratio between the chromatic components of the pump [28]. Previous work assumed that these APT bursts are linearly polarized [27, 28], yet we will show that this assumption is inaccurate.

Changing the polarization of one or both pump components from linear/circular to elliptic leads to so called bi-elliptical pumps [1, 15, 21, 37], which generally gives rise to elliptically polarized harmonic emission, with no particular symmetry constraints. Indeed, it was demonstrated that varying the ellipticities of the pump components can be used for tuning the ellipticity of the high harmonics [1]. The APTs are also modified in this scheme, but how? Specifically, what are the properties of the interlocked APTs that are associated with this ellipticity control? Does a simple mapping between the harmonic ellipticities and APTs properties exist?

Here we identify a regime of HHG driven by bi-elliptical pumps that leads to semi-analytical mapping between the ellipticities of the high harmonics and properties of the interlocked APTs. In this scheme, HHG is driven by a two-color pulse, a fundamental frequency and its second harmonic, where the two colors are slightly elliptically polarized with opposite helicity and perpendicular elliptical major axes. The ellipticities of the harmonics vary all the way from linear to circular when even small ellipticity is added to the crossed-polarized bi-chromatic field. In the time domain, the HHG radiation consists of two interlocked APTs that are not identical. The properties of the harmonic decompositions of each APT are also different. We show that the ellipticity of each harmonic order is determined by the following properties of the interlocked APTs harmonics decomposition: relative emission directions, relative time delay, and their ellipticities. We derive a semi-analytic formula that describes this mapping very accurately, allowing us to resolve these APTs features by measuring the high harmonics ellipticities only. We implemented this approach experimentally. This mapping between the harmonic's polarization and properties of the APTs may form a rich platform for polarization-resolved HHG spectroscopy, similarly to the highly successful delay scan between $\omega - 2\omega$ pumps [27, 28, 38].

We start by describing the scheme that gives rise to the semi-analytic mapping between the harmonics ellipticities and APT properties. Here, the HHG process is driven by co-propagating bi-chromatic $\omega - 2\omega$ fields that are orthogonally polarized. The field's polarizations may be linear or slightly elliptical, with equal ellipticities, opposite helicities, and perpendicular major axes. The relative phase between the two chromatic components is $\pi/2$. These slightly bi-elliptical pumps interact with an isotropic helium gas (s-type ground state).

We first present numerical results obtained using a quantum mechanical model (the HHG calculations are detailed in the supplemental material S1 (available online at stacks.iop.org/JPPHOTON/2/034005/mmedia)). The driving bi-elliptical orthogonal field, is given by:

$$\vec{E}(t) = \sqrt{\frac{I_0(t)}{1+\varepsilon_p^2}}\mathrm{Re}\left\{\sqrt{I_1}\left[e^{i\omega t}\left(i\varepsilon_p\hat{x}+\hat{y}\right)\right]+\sqrt{I_2}\left[e^{2i\omega t}\left(i\hat{x}+\varepsilon_p\hat{y}\right)\right]\right\} \quad (1)$$

where, $I_0(t)$ is the normalized pulse envelope, $I_{1,2}$ are the peak intensities of each component and $\varepsilon_p\left(-1 \le \varepsilon_p \le 1\right)$ is the ellipticity of the two components (with opposite helicities and perpendicular major elliptical axes).

Figure 1 shows HHG spectra calculated with linear $\varepsilon_p = 0$ (figure 1(a)) and slightly elliptical $\varepsilon_p = 0.019$ (figure 1(b)) drivers with $I_1 = I_2 = 1.8 \times 10^{18}$ W m^{-2} (see the supplemental material SM1 for numerical simulation details). The inset in each of these plots displays the Lissajous curves of the fundamental (red line), second harmonic (blue line) and joint (magenta) fields. In both cases, the HHG spectra consist of bright even- and odd-order harmonics with comparable strengths. The striking difference between these cases is in the ellipticity of the high harmonics. While the polarization of all the harmonics is linear when $\varepsilon_p = 0$, they become highly helical with the introduction of a small ellipticity to the driving field. For example, the ellipticities of the 34th and 35th harmonics are -0.77 and 0.31, respectively (the Lissajous curves of the 34th and 35th harmonics are shown in the right insets in figures 1(a) and (b)). Figures 1(c) and (d) show the emitted electric field, within one optical cycle, T, synthesized from harmonics 32–39 of the spectra shown in figures 1(a) and (b), respectively. In both cases, two elliptically polarized attosecond bursts with opposite helicities are emitted per optical cycle, forming interlocked APT pairs. Figures 1(e) and (f) show, respectively, the peak intensities and ellipticities of several harmonics from the plateau and cutoff regions (i.e. $I_q(\varepsilon_p)$ and $\varepsilon_q(\varepsilon_p)$, where q is the harmonic order) [39]. Clearly, the polarization of the high harmonics is extremely sensitive to minute changes in the pump's ellipticity, much more than the emission intensity (see the supplemental material SM2).

To understand the underlying mechanism for the large sensitivity of the harmonics ellipticity to the pump ellipticity, we numerically explore the time-frequency aspect of this scheme using Gabor transforms [40] of the emitted harmonic field (see the supplemental material SM1). We first present schematically in

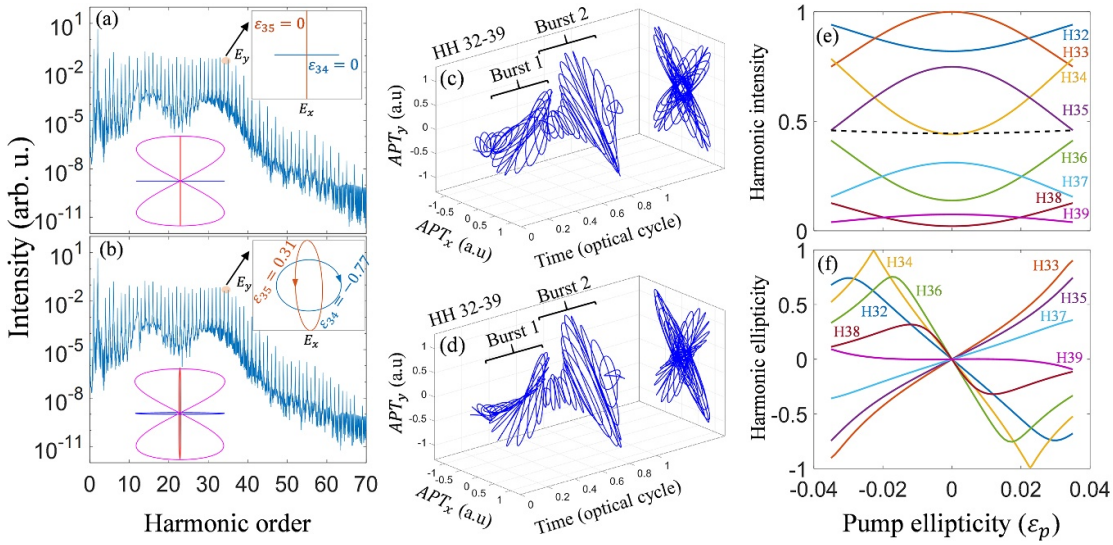

Figure 1. Calculated ellipticities and spectrum of high harmonics driven by slightly bi-elliptical orthogonal fields from helium (see the supplemental material SM1 for numerical simulation details). (a) and (b) HHG power spectra when the pump ellipticities are $\varepsilon_p = 0$ and $\varepsilon_p = 0.019$, respectively. The Lissajous curves of the corresponding separate fields (in red and blue) and the bi-elliptical field (magenta) are plotted/displayed below the spectrum. The Lissajous curves of the 34th and 35th harmonics are shown in the top right corners. Vectorial time-dependent field of harmonics 32–39 for (c) $\varepsilon_p = 0$ and (d) $\varepsilon_p = 0.019$. The emission consists of two attosecond bursts per optical cycle, each burst represents one APT of the interlocked APT pair. Intensities (e) and ellipticities (f) of harmonics 32–39 as a function of pump ellipticities $-0.035 \leq \varepsilon_p \leq 0.035$. The dashed black line in plot (e) corresponds to the averaged harmonic intensity. As shown, small modification in the pump leads to a significant variation in the polarization of the harmonics, while the change in the power spectra is moderate.

figure 2(a) the APT features that, as will be shown below, determine the ellipticity of the high harmonics and its dependence on the pump ellipticity. Each APT consists of elliptically polarized harmonics with ellipticities $\varepsilon_{1,q}$ and $\varepsilon_{2,q}$ (q is the harmonic order and 1, 2 denotes the APT order). Note that these APT harmonic ellipticities are different from the ellipticities of the full high harmonic radiation. For example, the high harmonics are linear for $\varepsilon_p = 0$ while the APTs and, as will be shown below, also the harmonics of each APT are elliptical. The angle between the major polarization axes of the burst harmonics is α_q. The delay between q-order harmonic compositions of the APTs are $T/2 + \delta_q$. Next we explore the dependence of these parameters ($\varepsilon_{1,q}$, $\varepsilon_{2,q}$, α_q and δ_q) on the pump ellipticity, ε_p (see supplemental material SM1 for the calculation description of these parameters). Figure 2(b) displays the dependence of the relative angle, showing that it is q-dependent [27, 35], but approximately independent of the pump ellipticity, within the explored range. Figure 2(c) displays the q-order harmonic ellipticities of each of the two APTs, i.e. $\varepsilon_{1,q}$ (solid line) and $\varepsilon_{2,q}$ (dashed lines present $-\varepsilon_{2,q}$), as a function of the pump ellipticity. The ellipticity of each burst is relatively small and approximately independent of the pump ellipticity, exhibiting very different behavior from the ellipticities of the full high harmonic radiation in figure 1(f). Figure 2(d) shows the phases between the consecutive bursts harmonics components versus harmonic order, termed ϕ_q. At $\varepsilon_p = 0$, the time delay between two consecutive bursts is $T/2$, which results in a phase of 0 and π for the even and odd harmonics, respectively (corresponding to $\exp(iq\omega T/2)$ factor in the Fourier transform). However, in contrast to the burst ellipticities and emission angles, the phase shifts exhibit significant dependence on the pump's ellipticity. It indicates (and will be confirmed below) that these shifts are the dominant source for the large sensitivity of the harmonics ellipticity to the pump ellipticity, as shown in figure 1(d).

We now analyze these phase shifts in greater detail. For each q-order harmonic component, we can intuitively formulate a phase in terms of attosecond-scale shifts, $\delta_q(\varepsilon_p)$, between the interlocked APTs as follows:

$$\phi_q(\varepsilon_p) = \pi q + 2\pi q \frac{\delta_q(\varepsilon_p)}{T}. \tag{2}$$

Interestingly, the temporal shifts are nearly uniform and linear with the pump ellipticity, across the harmonic's spectrum (figure 2(e)) and thus can be very well approximated by third-order Taylor expansion:

$$\delta_q(\varepsilon_p) = \beta_{1,q}\varepsilon_p + \beta_{3,q}\varepsilon_p^3 \tag{3}$$

where $\beta_{1,q}$ and $\beta_{3,q}$ are the first- and third-order Taylor expansion coefficients per harmonic order q. The second-order coefficient is removed because $\delta_q(\varepsilon_p)$ is an odd function that must change sign if the pump's

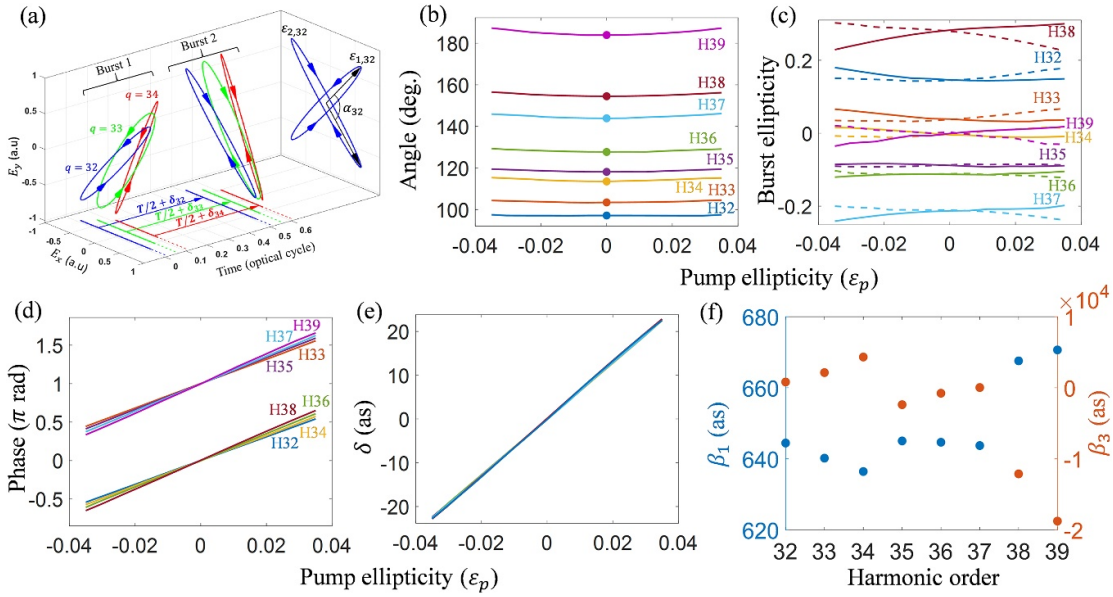

Figure 2. Time-frequency perspective. (a) Schematic illustration of the 32nd, 33rd and 34th harmonic fields. (b) Angle between the polarization axes of harmonic components of the two bursts, (c) ellipticities of several harmonic components of each of the two bursts, (d) relative phases of several harmonic components between the two bursts and (e) relative time shifts of several harmonic components between the two bursts as a function of pump ellipticity for harmonics 32nd (blue), 33th (brown), 34th (yellow), 35th (purple), 36th (green), 37nd (cyan), 38th (cherry) and 39results suggest that the polarizationth (violet) harmonics. (f) Calculated $\beta_{1,q}$ and $\beta_{3,q}$ variables according to equation (3) as a function of harmonic order.

helicity is inverted. Figure 2(f) shows the dependence of $\beta_{1,q}$ and $\beta_{3,q}$ on the harmonic order. The coefficients are largely independent of harmonic order in the plateau region (up to harmonic 37).

The above-presented numerical results suggest that the polarization of each harmonic order in figure 1(d) depends mainly on the (i) time shift between the two bursts (as described by equation (3)), (ii) the angle between consecutive bursts and (iii) the ellipticities of the bursts, where the last two variables are (approximately) independent of the pump ellipticity. If this is indeed the case, then all the ellipticity curves in figure 1(d) should be approximated by a general function of only four variables: $\beta_{1,q}$, $\beta_{3,q}$, $\alpha_q^0 = \alpha_q\left(\varepsilon_p = 0\right)$ and $\varepsilon_{b,q}^0 = \varepsilon_{1,q}\left(\varepsilon_p = 0\right)$. To verify this suggestion, we model the emitted q-order harmonic field to consist of harmonic components of two interlocked bursts (that are the unit cells of the interlocked APTs) by:

$$\vec{E}_q(t) = E_{0,q}\mathrm{Re}\left\{e^{iq\omega t}\left[\vec{d}\left(\varepsilon_{b,q}^0, -\alpha_q^0/2\right) + e^{i\phi_q\left(\varepsilon_p,\beta_{1,q},\beta_{3,q}\right)}\vec{d}\left(-\varepsilon_{b,q}^0, \alpha_q^0/2\right)\right]\right\}, \tag{4}$$

where

$$\vec{d}(\varepsilon,\theta) = \frac{1}{\sqrt{1+\varepsilon^2}}\left[\cos\theta\left(\hat{x} - i\varepsilon\hat{y}\right) + \sin\theta\left(i\varepsilon\hat{x} + \hat{y}\right)\right] \tag{5}$$

is the general expression for polarization state, ε is ellipticity and θ the angle between the polarization ellipse major axis and x direction. The ellipticity of the total harmonic-order field in equation (4) is given by (see derivation in the supplemental material SM3):

$$\varepsilon_q = \tan\left[\frac{1}{2}\arcsin\left[-2\frac{\mathrm{Im}\left(\chi_q\right)}{1+\left|\chi_q\right|^2}\right]\right], \tag{6}$$

where

$$\chi_q = i\tan\left[\frac{1}{2}\phi_q\left(\varepsilon_p,\beta_{1,q},\beta_{3,q}\right)\right]\frac{\sin\left(\alpha_q^0/2\right) + i\varepsilon_{b,q}^0\cos\left(\alpha_q^0/2\right)}{\cos\left(\alpha_q^0/2\right) - i\varepsilon_{b,q}^0\sin\left(\alpha_q^0/2\right)}. \tag{7}$$

Investigation of the role of the four variables in the analytic model is presented in the section SM5 in the supplemental material, showing that increasing the angle leads to increase (decrease) of the slope of the curve, i.e. the maximum ellipticity is obtained at smaller (larger) pump ellipticity, for even (odd) harmonic orders. The maximum ellipticity reaches ± 1, i.e. circular polarization, only when the burst's harmonic components are linearly polarized, and it decreases with increasing burst ellipticity. The slope of the curves increases with

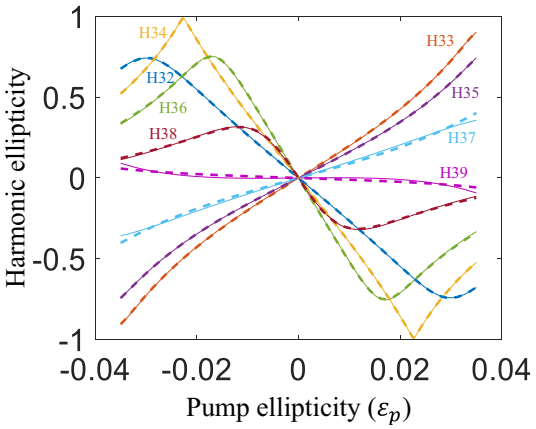

Figure 3. Calculated ellipticities of several harmonics as a function of pump ellipticity using TDSE (solid line) and semi-analytical model (dashed line) according to equation (6). The nearly perfect matching shows that the model captures the physics of HHG driven by slightly bi-elliptical pumps.

increase of the temporal shift δ_q, which is controlled by the pump ellipticity according to equation (3). According to the model, tuning the ellipticity of the pump beams induces attosesond-scale shifts between the emitted APTs, which gives rise to full control over the harmonics' polarization, from linear to circular.

Figure 3 shows a nearly perfect agreement between the curves calculated from equation (6) and time-dependent Schrödinger equation (TDSE). The variables for the analytical calculation are extracted directly from the TDSE calculation. The numerical and analytical curves coincide very well for harmonics in the plateau region and slightly deviate for cutoff harmonics. Clearly, the model captures the underlying mechanism for the HHG ellipticity in this geometry. We repeated this procedure for many harmonics order in different driving pulse parameters (including the variation of the pulse duration, envelope shape, laser intensity, and wavelength) and found a consistent match between the model and a full numerical calculation (see additional example in the supplemental material SM2). This universality indicates that it is possible to obtain the four variables of each harmonic order, $\beta_{1,q}$, $\beta_{3,q}$, $\alpha_q^0 = \alpha_q\left(\varepsilon_p = 0\right)$ and $\varepsilon_{b,q}^0 = \varepsilon_{1,q}\left(\varepsilon_p = 0\right)$, by measuring its ellipticity as a function of the pump ellipticity. For longer driving wavelength (see the supplemental material SM4), the variable $\beta_{3,q}$ can be neglected.

Next, we employ the derived model (equation (6)) to explore experimentally polarization-resolved high harmonic spectroscopy of the interlocked bursts. The experimental setup for measuring the high harmonics degree of circularity via the x-ray magnetic circular dichroism effect (XMCD) (for fully polarized light, the degree of circular polarization (DCP) corresponds to ellipticity as $\mathrm{DCP} = 2\varepsilon_q/\left(1+\varepsilon_q^2\right)$), is described in the section SM6 in the supplemental material.

Figure 4(a) presents the measured DCP for harmonic orders in the region of the Cobalt M-edge. We optimally-fitted equation (6) to the measured data (using weighted nonlinear-least square fit) for harmonics 34–37 for which Co is magneto-optically active, extracting the values of the four free variables, $\beta_{1,q}$, $\beta_{3,q}$, α_q^0 for each harmonic, and $\varepsilon_{b,q}^0$ for the even-order harmonics. The resulted curves are shown in figure 4(a) and the obtained values of the free variables are presented in table 1. We could not extract $\varepsilon_{b,q}^0$ of the odd harmonics because the ellipticity curves of such harmonics, i.e. odd harmonics with $\alpha_q^0 \approx 180°$, are too weakly influenced by these variables. Figure 4(b) presents the attosecond delays for the measured harmonics using the extracted $\beta_{1,q}$, and $\beta_{3,q}$. The shaded regions represent the error in the fitting procedure.

Figure 4(a) shows that the model captures well the main features of the experimental curves, hence equation (6) can be used to extract data on the emission process—in the form of the four measured variables for each harmonic order. Still, the deviations between the measured and model curves are larger than expected according to figure 3, especially for the odd harmonics. We associate these deviations to the possible effects of the interaction length, compared with a single atom effect, and the experimental error in phase delay of $\pi/2$ when sampling of the relative phase (2° rotation steps of the borosilicate slab).

The correspondence can be improved by refining the control over the phase between the pump components, measuring harmonic ellipticity in the plateau region rather than the cutoff region, and having the nonlinear medium in a gas jet instead of a gas cell (to avoid propagation effects).

To conclude, we identified an HHG scheme driven by cross-polarized $\omega - 2\omega$ slightly bi-elliptical pumps, in which the ellipticities of the high harmonics can be tuned from linear to circular. In the time domain, the HHG radiation consists of a pair of interlocked APTs. We mapped semi-analytically the ellipticity of a high harmonic to features of the APTs harmonic constituents: ellipticities, relative time delay and relative angle.

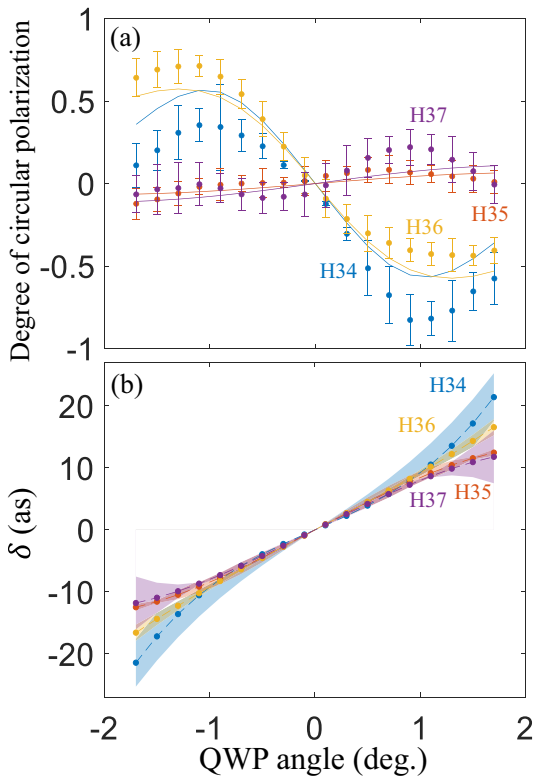

Figure 4. Experimental polarization-resolved spectroscopy of interlocked attosecond bursts. (a) Degree of circular polarization (normalized stokes parameter S_3/S_0) as a function of quarter-wave plate (QWP) angle for harmonics 34–37. Solid curves calculated according to equation (6) and variables from table 1 ($\varepsilon^0_{b,q}$ with q =35 and 37 that could not be extracted from the data were assumed to be equal to $\varepsilon^0_{b,q}$ with $q = 34$ and 36, respectively). (b) Extracted attosecond-scale shifts from the fitting procedure for measured harmonics (the shaded regions represent the error in the fitting procedure).

Table 1. Table of extracted interlocked APT variables. The angle between the polarization axes of the consecutive radiation bursts α, the ellipticity of the radiation burst ε^0_b, the 1st β_1 and 3rd β_3 coefficients of the Taylor expansion of the attosecond-scale delays between the two consecutive radiation bursts. The errors correspond to confidence of 68%.

Harmonic	H34	H35	H36	H37
α^0 (deg.)	150.6 ± 8.7	167.6 ± 6.8	136.3 ± 9.2	158.1 ± 12.7
ε^0_b	0.32 ± 0.07		0.41 ± 0.04	
$\beta_1 \times 10^2$ (as)	4.2	6.3	5.1	5.9
$\beta_3 \times 10^5$ (as)	3.4	-1.5	5.3	-1.4
R^2	0.88	0.46	0.95	0.43

We then demonstrated reconstruction of the properties of the interlocked APT pair from measurements of the harmonics' ellipticities. The high sensitivity of the HHG polarization to the ellipticity of a crossed-polarized bi-chromatic pump laser, as shown here, requires a careful look at past and future experiments that use such drivers. On one hand, careful analysis of the pump polarization should be made to avoid ellipticity artifacts, and on the other hand, mapping the harmonic's polarization onto the properties of the APTs opens a route for attosecond-resolved spectroscopy.

Acknowledgments

This work was supported by the by the Israel Science Foundation (Grant No. 1781/18) and the Wolfson Foundation. O N gratefully acknowledges the support of the Adams Fellowship Program of the Israel Academy of Sciences and Humanities.

ORCID iDs

Eliyahu Bordo https://orcid.org/0000-0002-6881-441X
Ofer Kfir https://orcid.org/0000-0003-1253-9372

Sergey Zayko https://orcid.org/0000-0001-9826-8627
Ofer Neufeld https://orcid.org/0000-0002-5477-2108

References

[1] Fleischer A, Kfir O, Diskin T, Sidorenko P and Cohen O 2014 *Nat. Photon.* **8** 543
[2] Kfir O *et al* 2015 *Nat. Photon.* **9** 99
[3] Ferré A *et al* 2015 *Nat. Photon.* **9** 93
[4] Hickstein D D *et al* 2015 *Nat. Photon.* **9** 743
[5] Fan T *et al* 2015 *Proc. Natl. Acad. Sci.* **112** 14206
[6] Lambert G *et al* 2015 *Nat. Commun.* **6** 6167
[7] Gruson V, Weber S J, Barreau L, Hergott J-F, Lepetit F, Auguste T, Carré B, Salières P and Ruchon T 2018 *JOSA* B **35** A15
[8] Ellis J L *et al* 2018 *Optica* **5** 479
[9] Huang P-C *et al* 2018 *Nat. Photon.* **12** 349–54
[10] Azoury D, Kneller O, Krüger M, Bruner B D, Cohen O, Mairesse Y and Dudovich N 2019 *Nat. Photon.* **13** 198–204
[11] Zuo T, Bandrauk A D 1995 *Nonlinear Opt. J. Phys. Mater.* **04** 533
[12] Eichmann H, Egbert A, Nolte S, Momma C, Wellegehausen B, Becker W, Long S and McIver J K 1995 *Phys. Rev.* A **51** R3414
[13] Long S, Becker W and McIver J K 1995 *Phys. Rev.* A **52** 2262
[14] Pisanty E, Sukiasyan S and Ivanov M 2014 *Phys. Rev.* A **90** 043829
[15] Kfir O, Bordo E, Haham G I, Lahav O, Fleischer A and Cohen O 2016 *Appl. Phys. Lett.* **108** 211106
[16] Dorney K M *et al* 2019 *Nat. Photon.* **13** 123
[17] Pisanty E, Rego L, San Román J, Picón A, Dorney K M, Kapteyn H C, Murnane M M, Plaja L, Lewenstein M and Hernández-García C 2019 *Phys. Rev. Lett.* **122** 203201
[18] Baykusheva D, Ahsan M S, Lin N and Wörner H J 2016 *Phys. Rev. Lett.* **116** 123001
[19] Jiménez-Galán Á, Zhavoronkov N, Schloz M, Morales F and Ivanov M 2017 *Opt. Express* **25** 22880
[20] Harada Y, Haraguchi E, Kaneshima K and Sekikawa T 2018 *Phys. Rev.* A **98** 021401
[21] Baykusheva D and Wörner H J 2018 *Phys. Rev.* X **8** 031060
[22] Kfir O *et al* 2017 *Sci. Adv.* **3** eaao4641
[23] Stremoukhov S, Andreev A, Vodungbo B, Salières P, Mahieu B and Lambert G 2016 *Phys. Rev.* A **94** 013855
[24] Mahieu B, Stremoukhov S, Gauthier D, Spezzani C, Alves C, Vodungbo B, Zeitoun P, Malka V, De Ninno G and Lambert G 2018 *Phys. Rev.* A **97** 043857
[25] Neufeld O, Podolsky D and Cohen O 2019 *Nat. Commun.* **10** 405
[26] Neufeld O and Cohen O 2019 *Phys. Rev. Lett.* **123** 103202
[27] Shafir D, Mairesse Y, Villeneuve D M, Corkum P B and Dudovich N 2009 *Nat. Phys.* **5** 412
[28] Shafir D, Mairesse Y, Wörner H J, Rupnik K, Villeneuve D M, Corkum P B and Dudovich N 2010 *New J. Phys.* **12** 073032
[29] Alon O E, Averbukh V and Moiseyev N 1998 *Phys. Rev. Lett.* **80** 3743
[30] Milošević D B and Becker W 2000 *Phys. Rev.* A **62** 011403
[31] Chen C *et al* 2016 *Sci. Adv.* **2** e1501333
[32] Kim C M and Nam C H 2006 *J. Phys. B: At. Mol. Opt. Phys.* **39** 3199
[33] Brugnera L, Hoffmann D J, Siegel T, Frank F, Zaïr A, Tisch J W G and Marangos J P 2011 *Phys. Rev. Lett.* **107** 153902
[34] Kitzler M and Lezius M 2005 *Phys. Rev. Lett.* **95** 253001
[35] Kitzler M, Xie X, Roither S, Scrinzi A and Baltuska A 2008 *New J. Phys.* **10** 025029
[36] Kitzler M, Xie X, Scrinzi A and Baltuska A 2007 *Phys. Rev.* A **76** 011801
[37] Bordo E, Neufeld O, Kfir O, Fleischer A and Cohen O 2019 *Phys. Rev.* A **100** 043419
[38] Dudovich N, Smirnova O, Levesque J, Mairesse Y, Ivanov M Y, Villeneuve D M and Corkum P B 2006 *Nat. Phys.* **2** 781
[39] Corkum P B 1993 *Phys. Rev. Lett.* **71** 1994
[40] Chirilă C C, Dreissigacker I, van der Zwan E V and Lein M 2010 *Phys. Rev.* A **81** 033412